Krka, Pharmaceutical Factory, Novo mesto, Slovenia

Crystal structure of indapamide determined from powered diffraction data

M. Smrkolj[1], A. Meden[2]

Received October 26, 2005, accepted March 19, 2006

Matej Smrkolj, Krka, d.d. Pharmaceutical Factory, Šmarješka cesta 6, SI-8501 Novo mesto, Slovenia
matej.smrkolj@krka.biz
Prof. Dr. Anton Meden, University of Ljubljana, Faculty of Chem. Technology, Aškertena 5, 1000 Ljubljana, Slovenia

Pharmazie 61: 999–1004 (2006)

Indapamide is used in the treatment of hypertension. In the European Pharmacopoeia it is specified that indapamide may contain up to 3 wt.% of water. On the basis of the results of thermal (TGA, DSC), DVS and X-ray powder diffraction analyses it has been supposed that this feature arises from the fact that indapamide exists in the form of a non-stoichiometric hydrate. The water molecules are only weakly and reversibly bound into the crystal structure. The major framework of the crystal structure, built of indapamide molecules, remains practically unchanged upon dehydration and/or hydration processes. In order to prove this hypothesis and understand the hydration-dehydration behavior, the as yet unknown crystal structure of indapamide needed to be determined. Since it was not possible to grow any adequate single crystals, we decided to solve the structure from laboratory X-ray powder diffraction data. The solved structure confirmed the hypothesis of weakly bound water in the voids between the indapamide molecules and also served as a basis to evaluate and explain the relative humidity dependence of the unit cell parameters of indapamide.

1. Introduction

The existing literature does not contain any data on the polymorphism of indapamide. Thus polymorphic changes may not be expected on heating indapamide or storing at increased relative humidity. However, this does not mean that special attention need not be paid to the behaviour of the active ingredient in the solid state; external factors may also affect the equilibrium of water in the indapamide structure. The European Pharmacopoeia (2005) states that indapamide may contain up to 3 wt. % of water. To elucidate the way in wich water molecules are bound into the crystal structure of indapamide, we used a series of techniques which enabled us to find and confirm an explanation for the indapamide – water equilibrium. To monitor this dynamic equilibrium more closely, we used thermal analysis (TGA – Thermo-Gravimetric Analysis, DSC – Differential Scanning Calorimetry), DVS (dynamic vapor sorption) and X-ray powder diffraction at various relative humidity values.

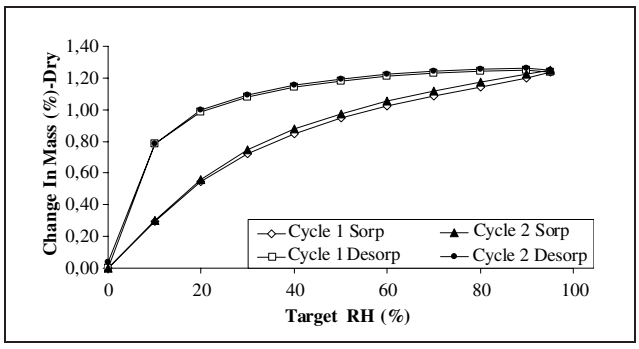

Fig. 1: DVS isotherm plot of unheated indapamide sample

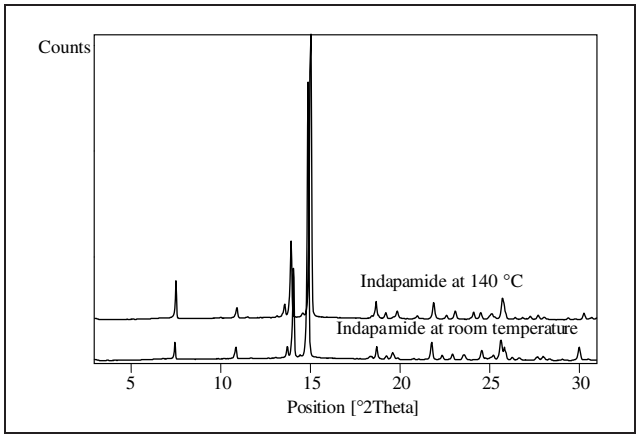

Fig. 2: XRPD patterns of an indapamide sample at room temperature and 140 °C

2. Investigations, results and discussion

2.1. Hydration-dehydration

TGA and especially DTGA (Derivative Thermo-Gravimetric Analysis) curves for indapamide do not show sharp maxima of weight loss, which suggests a continuous loss of water from the structure. Mass loss begins immediately after the temperature is raised above room temperature and subsequently the mass decreases steadily down to 115 °C when dehydration slows down and ceases at 160 °C (Figs. 1, 2). The entire mass loss amounts to

~2%. The DSC curve clearly shows that soon after complete dehydration, indapamide starts to melt (Fig. 3). A very broad endothermic effect extends over the same temperature region as water loss on the TGA curve. No additional endo/exothermic effects can be seen, which excludes phase alterations during dehydration. After complete dehydration, indapamide exists in an anhydrous form over a short temperature interval after which the structure begins to melt.

If indapamide is heated to the temperature of complete dehydration (160 °C), cooled and exposed to air for three days, and then resubmitted to TGA and DSC, both curves are very similar to those of previously unheated indapamide. This means that the dehydration is completely reversible and the sample can be completely rehydrated under room conditions. This is proved by Karl-Fischer titration of water in unheated and heated-cooled-room-exposed samples of indapamide. In both cases the water content is equal within the experimental error.

The affinity of the dehydrated structure for water is indicated even better under dynamic conditions of hydration-dehydration during the DVS experiment (Fig. 1). Indapamide shows greater affinity toward water at low RH than at higher RH. The hysteresis loop is widest at 10% RH and narrows at higher RH. These features as well as the amount of water absorbed indicate that the hydration of indapamide is not mere surface adsorption of water but is more likely to involve inclusion insertion in the crystal structure.

To verify this we performed two sets of X-ray powder diffraction scans, one at elevated temperatures and the other at room temperature, at varying relative humidity. Both experiments led to similar conclusions. No abrupt phase transition was observed on heating up to 140 °C and varying the RH from 10 to 90% at room temperature – the crystal structure remains stable under these conditions. However, some peaks in the diffraction patterns are observed to be shifted on heating-cooling or drying-moisturizing. The shifts are of the order of a few tenths of a degree 2Θ. The greatest peak shifts appear at 14°, 15° and 24° 2Θ. The largest shifts compared to the initial state are observed at the highest temperature of 140 °C (Fig. 2). Comparing the two sets of diffraction patterns, we established that drying the sample at room temperature has a similar effect (shifts the same reflections in the same direction) as heating the sample. This is obvious to some extent (heating causes dehydration), but one must bear in mind also the thermal expansion of the sample, which also shifts the reflections – not necessarily in the same direction as dehydration. From this point of view, the room temperature variable humidity experiment is more relavant to our problem. In particular, on the basis of its results, we may finally conclude, that the water is not just surface adsorbed/desorbed but is inserted into/removed from the crystal structure. The main part of the structure formed from the indapamide molecules adjusts only a little to accommodate the water molecules if they are present. This causes slight changes of the unit cell parameters, observed as peak shifts in the diffraction pattern. This is the only way to explain the peak shifts observed. The facts that the crystal structure does not collapse on dehydration/hydration and that this process is completely reversible, indicate that the framework of indapamide molecules in the crystal structure is rather rigid and water molecules are only weakly bound in the voids of this framework. To corroborate this hypothesis, we needed to know the crystal structure of indapamide.

2.2. Crystal structure

Unfortunately we were not able to grow suitable single crystals, so we had to undertake the determination of the crystal structure from powder data collected on the laboratory X-ray diffractometer. The positive aspect was that the molecule of indapamide is suitable for the determination of its crystal structure by direct-space Monte-Carlo/simulated annealing methods since it is rather rigid, which means here are anly a small number of variables to find. Considering only non-hydrogen atoms, indapamide has only three free parameters (torsion angles) while the remaining geometry of the molecule can be defined from existing knowledge (Allen et al. 1987).

Structure determination from powder diffraction data is a multi-step process that requires several types of data analysis (indexing, space group determination, structure solution and final refinement) (Meden 1998). To get the best results from our equipment we also chose a multiple data collection procedure.

First, a small sample of indapamide was spread in a very thin layer on a "zero background" sample holder and scanned in Bragg-Brentano geometry with settings set to the maximum resolution (see Experimental) in the range 4–37° 2Θ. Next, silicon powder was added to the sample as an internal peak position standard and the sample was scanned again on the same holder with the same configuration of the diffractometer. Using this procedure we reached the maximum resolution (due to the small thickness of the sample the transparency broadening was minimal) and reduced the zero-error as much as possible. These two facts are crucial for the first step of the structure determination – indexing the pattern (finding a true unit cell). Without successful indexing, one cannot proceed any further.

Careful data collection worked well in our case and with the help of the programs Crysfire (Shirley 1999), Treor (Werner et al. 1985) and Checkcell (Laugier and Bochu 2000) we found a reasonable unit cell with a high figure of merit. The unit cell was monoclinic ($a = 23.8$ Å, $b = 9.7$ Å, $c = 15.1$ Å, $\beta = 91.6°$) and indexed all observed reflections.

The next step was the space group determination. Considering the conditions of systematic reflection extinctions using the Checkcell program we ended up with four approximately equally probable space groups: P21/c, C2/c, C2/m and I2/a. A more definite decision was not possible due to reflection overlap at higher angles. Therefore we proceeded to the next step – structure solution – with all four possible space groups and tried to find a suitable structural model in any of them.

To solve the crystal structure, another X-ray diffraction pattern was used. As the crystallites were tiny plates, high preferred orientation was expected in the Bragg-Brentano data collection geometry. To reduce this problem, which could seriously reduce the probability of successfully solving the structure, we collected the powder pattern in transmission geometry with the sample mounted in a rotating capillary. The expected effect of morphological characteristics was confirmed by comparing diffraction patterns recorded in reflection and transmission geometry (Fig. 3). In reflection geometry the peak intensities are seriously affected by preferred orientation.

The Fox program (Favre-Nicolin and Cerny 2002) was applied to the transmission diffraction pattern to solve the crystal structure. Fox uses a direct space Monte Carlo simulated annealing (parallel tempering) global optimization method to find the correct position, orientation and confor-

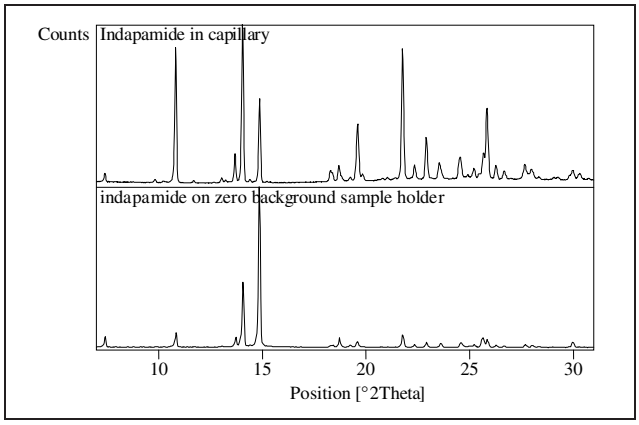

Fig. 3: Comparison of XRPD patterns recorded in reflection (zero background sample holder) and transmission (capillary) geometries

mation of atoms, molecules or fragments in the unit cell. The cost function (criterion to keep or reject the trial structure and to select the best one) is the match between the measured powder pattern and the one calculated from each trial structure.

In our case we knew the molecular structural formula and the simplest way to describe it as an input to Fox was as the Z-matrix. Hydrogen atoms, being very weak X-ray scatterers, were omitted and the conformation of the molecule then depended on only three free torsion angles (Fig. 4). All the rest are rigid fragments in which the bond lengths, bond angles and torsion angles are well defined by thousands of organic compounds (Allen et al. 1987). Thus there were only nine free variables: the position of the molecule in the unit cell (3 variables), its orientation (3 variables) and the three torsion angles.

With this input, the program was run for all the most probable space groups. On the basis of the numerical (R_{wp}) and visual match between the measured and calculated diffraction patterns as well as the stereochemical acceptability of the molecular conformation and the crystal-chemical acceptability of the molecular packing, it was clear that the best solution was obtained in the space group I2/a. In this space group we also tried to find a possible location of water molecules in the structure, but the attempts were unsuccessful. This was not surprising,

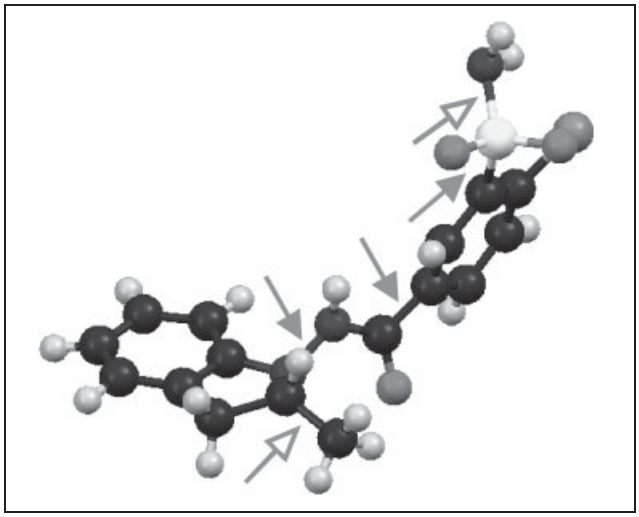

Fig. 4: Indapamide molecule. The arrows mark free torsion angles in the molecule. The empty arrows indicate the two free torsion angles involving only hydrogen atoms and thus not being applied for solving the structure

because of the very small scattering contribution of a water molecule compared to the indapamide molecule. Furthermore, according to TGA the water sites in the structure were most probably incompletely occupied (about 0.35 mole of water per one mole of indapamide – $C_{16}H_{16}ClN_3O_3S \cdot 0.35\,H_2O$), which means that the total scattering power of water was less than 2% and it is understandable that Fox was not able to locate it. Even without water the crystallographic model obtained (unit cell, space group, atomic coordinates) fulfilled all requirements rather well and it was ready for the last step in structure determination Rietveld refinement.

2.3. Rietveld refinement

Rietveld refinement is a least-squares based optimization of structural and profile parameters (from which the theoretical powder pattern is calculated) to minimize the difference between the calculated and measured powder patterns. It uses all crystallographic information present in the pattern. Unfortunately the information content in our pattern was rather low. We used the same data as for the structure solution, that is the diffraction pattern recorded in transmission. Due to poor crystallinity of the sample, the pattern showed peaks only up to 55° 2Θ. It was therefore out of the question to refine all the atomic coordinates independently (the number of variables would exceed the information content and the molecule would refine to nonsense). We used restrained refinement instead. This means that the bond lengths and angles that are well known from similar molecules were soft restrained (for details see Baerlocher 1995) and only the position, orientation and five torsion angles were free. This was similar to the Fox input, the difference being in the algorithm, which is in Rietveld refinement programs dedicated to fine extraction of the information from the profile. The algorithm in Fox is optimized for fast calculations and finding rough models. Furthermore, hydrogen atoms were added in their theoretical positions and this caused two additional torsion angles to be refined.

For the Rietveld refinement we used the TopasR program (Topas 2000). The weights of the above mentioned restraints against the diffraction pattern were optimized to give as much influence as possible to the pattern while still keeping the molecular geometry reasonable. A pseudo-Voigt function was used to describe the peak profile and peak asymmetry was taken into account in applying the axial divergence model. Altogether we refined the following variables: background parameters – Chebyshev polynomial (10), zero error (1), peak profile – Pseudo-Voigt (6), peak asymmetry – axial divergence (3), unit cell (4), atomic coordinates (120), overall isotropic atomic displacement factor B (1) and scale factor (1). We applied 125 soft restraints to inter-atomic distances which act as additional observations in the refinement (for details see Baerlocher 1995). We finally reached an R_{wp} of 9.1%, which already means a good match between calculated and observed patterns.

At this point we again explored the possibility of locating the water molecules in the crystal structure. The *Atoms* program (Dowty 2002) was used to calculate the cavity shapes and locations in the as-refined crystal structure with indapamide only. In fact it was found that only two cavities exist that could potentially host water molecules. One "pocket" is formed between four indapamide molecules and is surrounded by a methyl group and four aromatic fragments of different molecules, The other void is

located on the twofold axis surrounded by $-SO_2NH_2$ groups of two different molecules. In several refinement trials a water molecule was put into one or both suitable cavities and its position, orientation and occupancy were refined. The results showed that water is only present in the hydrophilic pocket between the two amide groups. The other, hydrophobic, pocket is empty and becomes smaller when the water molecule is included in the hydrophilic one due to relaxation of the indapamide molecules during refinement. The occupancy parameter of the water molecule refines to 0.34(8), which is in very good agreement with the expected value of around 0.35 calculated from the weight loss in the TGA (1.7%). Adding water to the structure resulted in 5 more parameters (y coordinate of oxygen x, y, z coordinates of hydrogen (the other hydrogen atom is created by the two-fold axis) and the population parameter and 2 more restraints (O−H distance and H−O−H angle). The final fit of the calculated and measured patterns is significantly better with the water molecule added into the structure ($R_{wp} = 5.6\%$, Fig. 5) and the crystal-chemical environment of the water is reasonable − two hydrogen bonds of 2.6(1) A to amide nitrogen atoms. We consider this as the final proof for crystallographically bound water in indapamide.

The final crystallographic parameters are given in Tables 1 and 2. A kind of dimer can be seen, where two molecules of indapamide are bound by π-π interaction between the two parallel aromatic rings at a distance of about 3.5 A. In addition, the two molecules in forming the dimer are connected with a weak hydrogen bond of 3.13(9) Å between the peptide nitrogen and peptide oxygen atoms. Dimeric units are arranged in layers normal to the crystallographic axis a and the water molecules are located between the layers (Fig. 6).

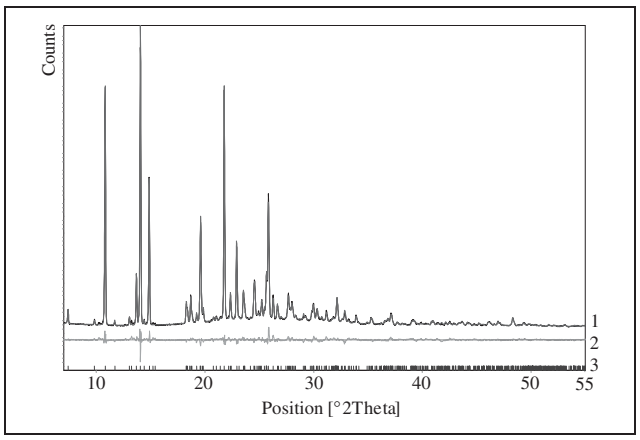

Fig. 5: Final Rietveld plot − Calculated (1) and measured (2) patterns and their difference (3). Vertical bars represent reflection positions

Table 1: Crystal data

CAS number	26807-65-8
Formula	$C_{16}H_{16}ClN_3O_3S \times 0.35\,H_2O$
Formula weight (g)	372
Crystal system	monoclinic
Space group	I 1 2/a 1 (15)
Z	4
a (Å)	23.811(3)
b (Å)	9.6940(9)
c (Å)	15.114(2)
β (°)	91.66(3)
V (Å^3)	3487(3)
R_{wp} (%)	5.6

Table 2: Atomic coordinates and isotropic atomic displacement factors

C1	0.490(5)	0.720(8)	0.727(7)	5.2
N2	0.534(4)	0.632(8)	0.741(4)	5.2
N3	0.583(4)	0.667(7)	0.699(6)	5.2
C4	0.629(6)	0.686(2)	0.765(7)	5.2
C5	0.601(2)	0.572(2)	0.638(7)	5.2
C6	0.569(4)	0.498(2)	0.579(2)	5.2
C7	0.596(1)	0.412(2)	0.521(8)	5.2
C8	0.654(1)	0.405(2)	0.522(9)	5.2
C9	0.685(4)	0.471(2)	0.588(2)	5.2
C10	0.658(1)	0.562(2)	0.641(7)	5.2
C11	0.683(5)	0.638(2)	0.718(9)	5.2
C12	0.633(5)	0.815(2)	0.821(7)	5.2
O13	0.498(2)	0.834(5)	0.699(3)	5.2
C14	0.437(6)	0.692(2)	0.770(9)	5.2
C15	0.389(9)	0.746(9)	0.733(5)	5.2
C16	0.436(5)	0.620(2)	0.848(9)	5.2
C17	0.338(6)	0.702(2)	0.764(9)	5.2
C18	0.337(5)	0.62 (1)	0.839(9)	5.2
C19	0.385(7)	0.581(8)	0.880(5)	5.2
Cl20	0.273(9)	0.594(2)	0.885(2)	5.2
S21	0.386(2)	0.476(4)	0.975(2)	5.2
O22	0.443(2)	0.438(5)	0.995(3)	5.2
O23	0.367(2)	0.559(5)	0.047(3)	5.2
N24	0.348(4)	0.340(9)	0.964(6)	5.2
H25	0.533(4)	0.565(5)	0.791(4)	5.2
H26	0.621(3)	0.633(6)	0.819(3)	5.2
H27	0.601(2)	0.877(6)	0.805(4)	5.2
H28	0.632(3)	0.791(8)	0.884(4)	5.2
H29	0.669(3)	0.863(6)	0.809(4)	5.2
H30	0.706(3)	0.716(5)	0.699(4)	5.2
H31	0.706(3)	0.576(6)	0.755(4)	5.2
H32	0.726(2)	0.468(6)	0.588(5)	5.2
H33	0.673(4)	0.362(6)	0.472(3)	5.2
H34	0.574(4)	0.364(6)	0.474(4)	5.2
H35	0.528(3)	0.503(6)	0.579(4)	5.2
H36	0.390(4)	0.787(6)	0.673(4)	5.2
H37	0.303(2)	0.731(6)	0.734(5)	5.2
H38	0.470(3)	0.611(6)	0.885(4)	5.2
H39	0.344(5)	0.297(7)	0.023(5)	5.2
H40	0.310(4)	0.365(8)	0.940(4)	5.2
O41	0.25	0.240(2)	0	8
H42	0.2(1)	0.3(3)	1.0(3)	8

Atomic displacement factors were set to be equal for all atoms in indapamide molecule and equal for water atoms, the latter were not refined

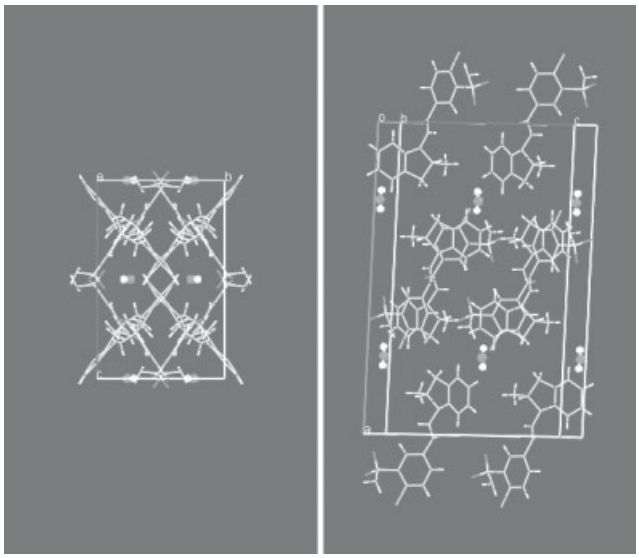

Fig. 6: Unit cell wiew down crystallographic a (left) and b (right) axes water molecules (emphasized by "ball&stick" plotting style) are located between the layers

2.4. Unit cell dependence on relative humidity

Values of the unit cell parameters of indapamide calculated at different values of relative air humidity are given in Table 3. These were determined with the Topas program using diffraction patterns recorded at different values of relative air humidity. As we were interested only in unit cell variations, the patterns were fitted without the structural model and the reflection intensities were refined to the best fit. The graphs in Fig. 7a–d show the dependence of the unit cell parameters on air humidity. The edges a and b increase with increasing quantity of water in the structure, while the edge c and the angle β (d) decrease. These changes are in accordance with the location of water molecules in the structure. The basic influence of water is shown with respect to parameter a. If the water molecules are present, the above mentioned layers, normal to a, are more widely separated. The other changes are due to relaxation of the packing of indapamide molecules, followed by the principal effect of increasing/decreasing the interlayer distance.

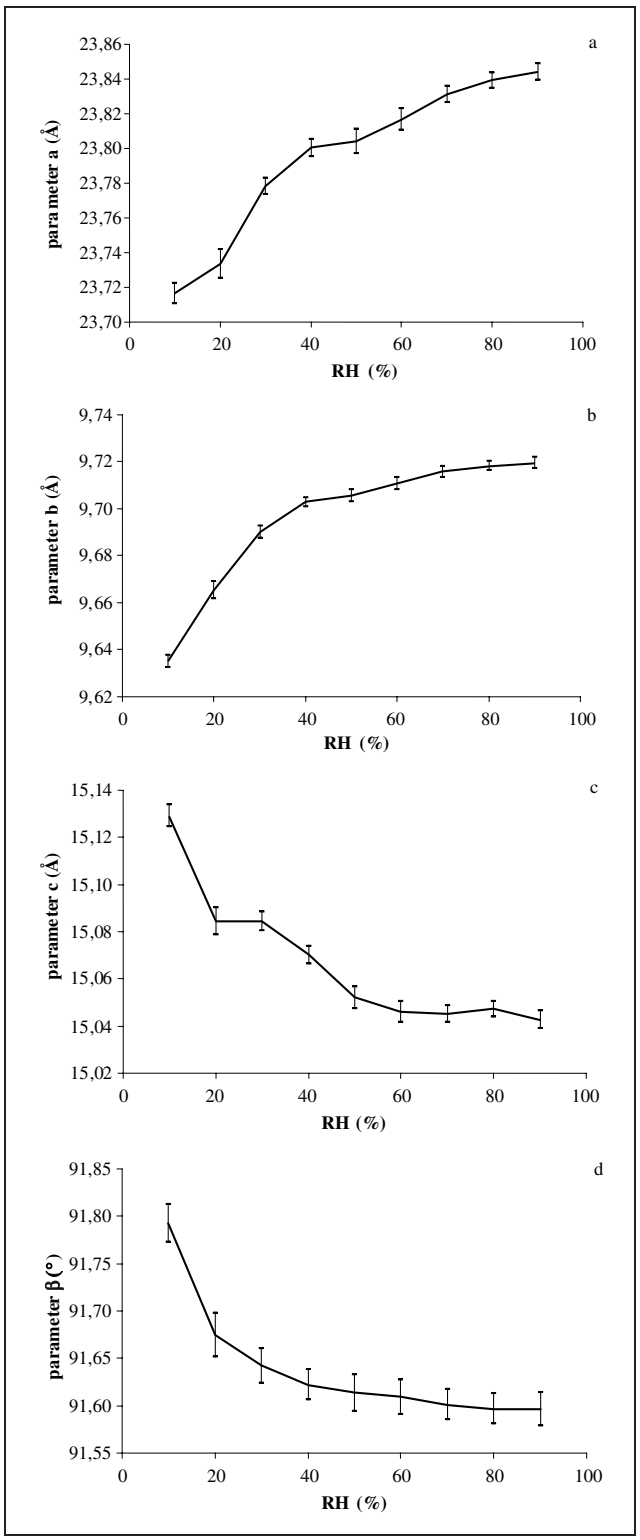

Fig. 7: Dependence of unit cell parameters of indapamide on relative air humidity at room temperature

Table 3: Values of the unit cell parameters calculated at different relative air humidities

RH [%]	parameter a [Å]	parameter b [Å]	parameter c [Å]	parameter β [°]	Volume [Å^3]
10	23.717(6)	9.635(3)	15.129(5)	91.79(2)	3455(2)
20	23.734(9)	9.665(4)	15.084(6)	91.67(3)	3459(2)
30	23.778(5)	9.690(3)	15.084(4)	91.64(2)	3474(2)
40	23.800(5)	9.703(3)	15.070(4)	91.62(2)	3479(2)
50	23.804(7)	9.705(3)	15.052(5)	91.61(2)	3476(2)
60	23.817(6)	9.711(3)	15.046(5)	91.61(2)	3478(2)
70	23.831(5)	9.716(3)	15.045(4)	91.60(2)	3482(2)
80	23.839(5)	9.718(3)	15.047(4)	91.60(2)	3485(2)
90	23.844(5)	9.719(3)	15.043(4)	91.60(2)	3485(2)

Even more instructive are plots of the dependence of the unit cell parameters on the absolute content of water in the structure. The latter was determined from the DVS experiment. The dependence is quite close to linearity (Fig. 12) and can be used to determine an approximate content of water in indapamide by calculating its unit cell without destroying or changing (drying, moisturizing) the sample. Only a reliable measurement of an X-ray powder diffraction pattern is required. This procedure may even work when indapamide is mixed with other material, but in this case the indapamide would have to be the major phase in the sample and the estimation would be approximate. This possibility was not pursued further as it is beyond the scope of this work.

3. Experimental

3.1. Sample preparation

The samples analyzed were chromatographically pure and not optically active.

3.2. Methods

3.2.1. Differential Scanning Calorimetry

The calorimetrical measurements were performed with a Perkin-Elmer DSC-2 differential scanning calorimeter. The mass of the sample was about 3 mg and the scanning rate was 10 °C/min in a nitrogen atmosphere. The DSC was calibrated with indium at the same heating rate as the samples.

3.2.2. Thermogravimetry (TG)

TG curves were recorded with a Perkin Elmer TGA 7 Thermogravimetric Analyser. Samples of approx. 20 mg were heated under a nitrogen atmosphere with a heating rate of 10 °C/min.

3.2.3. X-ray powder diffraction

X-ray powder diffraction patterns were measured on a Philips PW3040/60 X'Pert PRO diffractometer equipped with an X'Celerator detector using CuK_α radiation ($\lambda = 1{,}541874$ Å). Samples in the Bragg-Brentano geometry were scanned in a 2Θ range of 3–31° and a step size of 0.0167°. The X-ray powder diffraction patterns at elevated temperatures were performed on the same instrument equipped with a TTK and THC chambers. Samples in capillary geometry were scanned with a parallel beam (parabolic mirror) over a range of 7–55° 2Θ.

3.2.4. Dynamic vapor sorption (DVS)

The DVS measurements were performed with a Surface Measurement Systems Ltd DVS-1 at room temperature (25 °C) in a nitrogen flow (200 ml/min).

3.3. Computer programs

X'pert Highscore (X'pert HighScore 2005) – comparison of XRPD patterns (powder diffraction data visualisation). Crysfire (Shirley 1999) – indexing of the powder diffraction pattern (finding the unit cell). Treor (Werner et al. 1985) – alternate approach to powder pattern indexing (a semi-exhaustive trial-and-error powder indexing program for all symmetries). Checkcell (Laugier and Bochu 2000) – space group determination. Fox (Favre-Nicolin and Cerny 2002) – solving the crystal structure (a modular approach to *ab initio* structure determination from powder diffraction). TopasR (Topas 2000) – Rietveld refinement. Atoms (Dowty 2002) – cavity shapes calculation. Mercury (Mercury 2005) – crystal structure visualisation.

References

Allen FH, Kennard O, Watson DG, Brammer L, Orpen AG, Taylor R, (1987) Tables of bond lengths determined by X-ray and neutron diffraction. Part 1. Bond lengths in organic compounds. J Chem Soc Perkin Trans. II 12: S1–S19.

Baerlocher C (1995) Restraints and constraints in Rietveld method. In: Young RA (ed.) The Rietveld method, International Union of Crystallography, Oxford University Press Inc. New York, pp. 186–196.

Dowty E (2002), Atoms, Shape software, Kingsport, USA.

European Pharmacopea (2005), http://online.pheur.org/entry.htm

Favre-Nicolin V, Cerny R (2002) FOX, 'free objects for crystallography': a modular approach to *ab initio* structure determination from powder diffraction. J Appl Cryst 35: 734–743.

Laugier J, Bochu B CHECKCELL: a Software Performing Automatic Cell/Space Group Determination. Collaborative Computational Project, Number 14 (CCP14), Laboratory of Materials and Phyisical Engineering, School of Physics, University of Grenoble, France.

Meden A (1998) Crystal structure solution from powder diffraction data state of the art and perspectives. Croat Chem Acta 71: 615–633.

Mercury, Software for Crystal Structure Drawing and Visualisation, Cambridge Crystallographic Data Centre, 2005 (support@ccdc.cam.ac.uk).

Shirley R (1999) CRYSFIRE: a powder indexing suite. Collaborative Computational Project, Number 14 (CCP14), School of Human Sciences, Surrey, UK.

TOPASR V2.0, User Manual, Bruker AXS, Karlsruhe, Germany, 2000.

Werner P-E, Eriksson L, Westdahl M (1985) TREOR, a semi-exhaustive trial-and-error powder indexing program for all symmetries J Appl Cryst 18: 367–370.

X'pert HighScore, PANalytical b.v. Almelo, Netherlands, 2005.